AIMS Mathematics, 11(6): 18304–18328.
DOI: 10.3934/math.2026744
Received: 20 January 2026
Revised: 20 March 2026
Accepted: 30 March 2026
Published: 22 June 2026

https://www.aimspress.com/journal/Math

Research article

A mathematical model and its solutions for traffic flow management

Tiziana Campisi, Angela Ricciardello*, Marianna Ruggieri* and Giorgia Vitanza

University of Enna "Kore", Department of Engineering and Architecture, Cittadella Universitaria—94100 Enna, Italy

* **Correspondence:** Email: angela.ricciardello@unikore.it; marianna.ruggieri@unikore.it.

Abstract: The study of mathematical modeling of traffic flow has become increasingly important in modern urban contexts, driven by the need to enhance the quality of life in cities, mitigate environmental pollution, and improve the efficiency of transportation systems. Over the past decades, numerous mathematical frameworks have been proposed to characterize traffic dynamics, including microscopic, macroscopic, and kinetic models. Each of these approaches exhibits distinct strengths and limitations, which are typically associated with the computational complexity required for numerical simulations and with the capability of the model, to accurately reproduce real-world traffic phenomena, specifically, capturing complex interactions—such as those between pedestrians and vehicles—as well as emergent phenomena, such as queue formation at traffic signals, poses a significant challenge. In this study, we investigated the Riemann problem associated with the non-homogeneous Aw–Rascle model. More specifically, we conducted a systematic comparison of different numerical methods for solving the Riemann problem within this framework, with the aim of evaluating their performance and reliability.

Keywords: mathematical model; sustainable mobility; traffic flow; Riemann problem; Aw-Rascle model
Mathematics Subject Classification: 35L40, 35A09

1. Introduction

In recent years, the issues of pollution and climate change have become increasingly complex and urgent to address, to improve our quality of life and safeguarding the future of the planet. Since people and goods move mainly by road using polluting, noisy, and bulky vehicles (cars, motorbikes, trucks, and vans), mobility is one of the most complex problems related to environmental pollution that modern society must tackle. The interest of many scholars has therefore turned to the study of sustainable local mobility models, in accordance with the 2030 agenda [1]. The importance of integrating sustainable

mobility into future policies is increasingly recognized at the global level. The transition to low- or zero-emission transportation is a prerequisite for achieving the goal set by the Paris Agreement (2016) of limiting global temperature rise this century to "well below" 2 °C above pre-industrial levels (while pursuing a further 1.5 °C limit). From this perspective, cities will play a key role, as they house growing populations and the major activities that generate mobility demand. The literature shows that a variety of methodologies and strategies can be used to study this pressing issue. Various disciplines (i.e., threshold theory, cluster analysis, multi-criteria analysis, etc.) and methodological choices for evaluating sustainable mobility models can contribute in this direction [2, 3]. However, although there are several publications that have dealt with the degree of maturity of smart cities over time (see [4] and references therein for a review), relatively few researchers on evaluating of the maturity of sustainable mobility.

In this context, various disciplines propose complementary approaches, ranging from advanced vehicle technologies to infrastructure optimization [5]. For instance an graph-based approaches, such as the heterogeneous graph embedding model proposed by Li et al. [6, 7], highlight the importance of spectral properties in the analysis of complex systems. A similar perspective can be adopted in realistic traffic flow modeling to decompose the original Riemann problem into a set of local problems defined at each road junction.

Moreover, mathematical modeling plays a key role in simulating traffic dynamics and in systematically evaluating the impact of urban scenarios. The mathematical models developed for traffic flow applications can be classified into different categories, such as microscopic, macroscopic, and kinetic models (see [8]). Focus of this study lies on the numerical methods applied to solve a particular model based on the Aw-Rascle model in the nonhomogeneous case (see [9], where the generalized Aw-Rascle model in a multilane traffic case and the existence of global-in-time measure-valued solutions are described). A comparison among the Upwind method, the Lax-Wendroff, and the Beam-Warming method is proposed, to suggest the most suitable method for different cases of the Generalized Riemann Problem for which an exact solution is not available.

The paper is outlined as follows: In Section 2, we give a review of the major mathematical models in the context of traffic flow or pedestrian evacuation and their classification in macroscopic, mesoscopic and microscopic scales according to the scale of the scenario. In Section 3, the major advantages and drawbacks of each approach are listed. The model is described in Section 4, the numerical approaches are recalled in Section 5, and a comparison through numerical simulations is presented in Section 6.

2. Mathematical models for traffic flow and pedestrian dynamics

Traffic flow and pedestrian dynamics are important topics to study for several reasons, including the reduction of pollution, the optimization of travel times in urban areas, and the simulation of scenarios aimed at identifying effective strategies to improve cities for vehicles and pedestrians.

In parallel, within the context of tactical urbanism, strategies have been proposed to make cities more suitable and comfortable for pedestrians rather than cars. Including the introduction of parklets, which are spaces dedicated to pedestrians that occupy areas of the roadway traditionally used for parking (see [5] for further details on parklets).

This type of road intervention motivates the investigation of traffic flow and pedestrian dynamic models, with the aim of developing an integrated framework that accounts for vehicle flow, pedestrian

behavior, and their interactions.

2.1. Macroscopic scale

The macroscopic mathematical models presented in this paragraph are models based on fluid dynamic equations and, systems of partial differential equations. The latter are classified as first and second order models, namely, macroscopic models constituted by one or two partial differential equations, respectively. In particular, we focus on the Aw-Rascle model with Riemann initial conditions, because under a suitable hypothesis, the problem admits exact solutions.

2.1.1. First and second order models based on fluid dynamic equations

The standard example of the traffic first order macroscopic model was given by Lighthill and Whitham in 1955 [10] and Richards in the same year, but independently [11]. The model is expressed by the following partial differential equation

$$\frac{\partial \rho}{\partial t} + \frac{\partial(\rho v(\rho))}{\partial x} = 0,$$

where ρ is the density and $v(\rho)$ is the velocity depending on the density.

In [12], a generalization to the two dimensional case of the first order model was introduced by Hughes in 2002.

In [13], different macroscopic models are devised. These are compared and analytic considerations and numerical simulations are conducted to verify the correct reproduction of lane formation, evacuation room, etc. The feature that all the models have in common is the utilization of nonlocal conservation laws.

In [14], a macroscopic model that reproduces the Braess paradox for pedestrians and shows the global existence of nonclassical shock waves for a real problem, is devised. In [14], the focus is a panic situation in which the increase of the flow over the maximal possible in a "normal" situation, is taken into account, and a nonclassical Riemann solver is used.

The classic example of traffic second order macroscopic model was presented in 2000 by Aw and Rascle [15] and is mentioned in Section 4. In [16], the Aw-Rascle macroscopic model of car traffic modified into a two-way multi-lane model of pedestrian traffic is proposed. The most important contribution of this last paper is to provide a methodology to handle the congestion constraint in pedestrian traffic models. Congestion effects reflect the fact that the density cannot exceed a limit density corresponding to contact between pedestrians. They proposed to treat them by a modification of the pressure relation, which reduces the pedestrian velocities when the density assumes its maximal value.

In [17], three macroscopic continuum models are proposed, based on the microscopic model in which the vision based approach for the avoidance of collision is used [18]. In [19] they are analyzed and solved through a free mesh numerical method. This last example underlines the fact that the classification of the models is not very rigid, though hybrid models can be developed.

2.2. Microscopic scale

The microscopic mathematical models presented in this paragraph are the agent based models, in particular the cellular automata model and the force based models. The first class of models,

through to the definition of some logical and realistic rules, reproduces the actual behavior of the agents considered in the model (vehicles or pedestrians); the force based models, instead, use the dynamics equations to simulate the evolution in time of the traffic on a road or crowd in a room.

2.2.1. Cellular Automata

In the context of the microscopic scale mathematical models, in this subsection, the cellular automata model is illustrated.

The first one to use the term "cellular automata" was John Von Neumann [20] in 1950; he devised this kind of model but for different reasons with respect to the traffic flow or pedestrian dynamic. The term "cellular automata" refers to the self-reproduction of cells in a biological context. This kind of model was spread in the following years by John Horton Conway in his work about the game of life presented by Martin Gardner in [21]. In recent years, this model has been used and applied to a very large range of topics, from biology to the description of nature to pedestrian dynamics, which we are interested in.

In a mathematical setting and in the context of evacuation problems, we can define the cellular automata model as a discrete dynamic system constituted by a discrete time, a discrete space, and a limited number of possible states that vary following certain rules [22,23]. In particular, the description of the interaction among pedestrians is possible through the definition of a local function.

The cellular automata models can be classified in different ways, including space grid shape (square, triangle, hexagon variations,) the time evolution (synchronous or asynchronous), the number of states and the factor they take into account, and the evolution rules depending on the direction to which the pedestrian wants to go, usually with a fixed velocity, among possible directions that are defined by the neighboring cells (the Moore or the Von Neumann neighborhood are the most used).

Three groups of cellular automata models can be individualized depending on the coupling mechanism that is used to calculate the transition probability (see [23] and the references therein for further details):

- The lattice gas model in which a favorite direction is defined for each pedestrian, such that at each time steps, every direction, which has the same probability to be chosen except for the favorite direction, which has a higher probability.
- The floor field model, which is based on the idea of following the group preferences and describing a herding behavior in which the common goal of the crowd is to choose the shortest path to reach the exit.
- The other field based model, among which one can cite the Electrostatic-induced potential field model based on Coulomb's law. It describes the interaction between two pedestrians, treated as charged particles, that are attracted to the exit and repulsed by the walls and obstacles. The cost potential field, which is defined to minimize the cost of moving for each pedestrian, takes into account some psychological aspects of the crowd.

The application of cellular automata models in the context of evacuation problems is very spread but there are other examples of applications more suitable for our goal. The first example of a traffic flow model with cellular automata can be found in [24], from 1992.

Another example is in [29], where the highway traffic is simulated using the cellular automata model for different cases, such as single line or double line modeling. Four rules are used for the

cellular automata algorithm: Acceleration, deceleration, randomization, and move.

In [30], the effects of changing orders in the update rules on traffic flow are discussed. If an accident simulation has to be included in the model, one can set the velocity equal to zero for a slot of time for the vehicles in the neighborhood at the accident location. If we want to simulate the different phases of traffic, splitting it into free flow and congested flow, divided by a critical density and adding new rules for velocity is preferred. Additionally, the boundary conditions can be modified, passing from a less realistic closed system to a more realistic case with open boundaries with a certain probability that a car enters or leaves the studied road. We should also consider fact that on highway streets, the cars can switch lane, which is considered in [29].

In [31] a review of other applications of this kind of model (Agent based models to which cellular automata belong) for traffic flow simulations is reported.

2.2.2. Force based models

The force based models are another class of microscopic scale mathematical models [32–34]. The main idea that characterizes them is to treat the vehicles and/or pedestrians as particles whose movements and interactions follow the Newton-like laws of dynamics; thus, a system of second order Ordinary Differential Equations (ODEs) will arise from these considerations. The number of equations is equal to the number of microscopic elements considered. The forces that regard the vehicles and/or pedestrians are not exactly the ones used in a physical setting for Newton's Laws for this reason, they are called social forces [35, 36]. In this context, the word "force" stands for the "motivation to move or make a decision".

In [37], the intrinsic problems of the force based models are underlined. In particular, the action-reaction law that holds in the dynamics of particles is no more suitable for pedestrians. To fix this problem, some repulsive forces have been introduced in the model; however, on one hand, if the force is too high, some unrealistic oscillations will be reproduced; on the other hand, if the repulsive force is too low, the overlapping of pedestrians will be observed. Another issue arises from the analogy between a pedestrian and a particle. Indeed, a pedestrian should be represented as a volume in three dimensional space instead of a particle that could be a point in the plane. Moreover, a particle interacts with other particles in an isotropic way, while a pedestrian, who has more attention to the space in front of them, displaying anisotropic behavior. In [37], the authors suggested solutions in the form of the generalized centrifugal force model combined with accurate modeling of the 2-D projection of the human body using ellipses with velocity dependent semi-axes.

In [38], the interested reader can find an overview of the force based models with a historical excursus until current improvements. Indeed, to solve the unrealistic behaviors arising from the force based models, such as pedestrian overlapping or local oscillations or tunneling effects, other models were developed after the 2000s as velocity based models, data driven models, and hybrid models, in which the forces are mixed with the neural networks setting.

2.3. Mesoscopic scale

The mathematical models in the mesoscopic scale are mainly kinetic models, namely models based on the equations of the kinetic theory for gas dynamics. Usually, the Boltzmann equation is used, but a proper collisional term is on the right side of the equation, to take into account the different natures

and dynamics of the particles in a gas with respect to individuals in a crowd or vehicles in traffic.

2.3.1. Kinetic models

The kinetic models for traffic flows are introduced by Prigogine in [39]. The most used equation in this context is the Boltzmann equation:

$$\frac{\partial f}{\partial t} + \vec{v} \cdot \nabla_{\vec{x}} f + \vec{F} \cdot \nabla_{\vec{v}} f = C,$$

where f is the distribution function dependent on the position $\vec{x}$, the time is t, the velocity is $\vec{v}$, $\vec{F}$ is an external force, and C is the collision term.

In [40], an example of a kinetic model mixed with the game theory is proposed. The kinetic part enters the Boltzmann partial differential equations on the left, while the game theory and the probability theory are taken into account on the right of the equations, in which the "collision" term is defined. An important feature of this paper is the granular nature introduced to the equations, by introducing the velocity classes. This idea makes the model more realistic since the traffic flow is usually described as a "continuum", but in reality, it has a discrete nature.

In [41], a fully discrete kinetic model is introduced, with the novelty of the generalized kinetic theory inserted in the modeling approach.

In [42, 43], the continuity of the traffic flow is taken into account as a critical point of the kinetic models. Daganzo underlines the unjustified utilization of the distribution function in this context because of the low number of vehicles in a street with respect to the context of the kinetic theory in a physical setting.

In [44], a review of kinetic models for traffic flow is presented.

The literature on crowd modeling is limited to the approaches at the microscopic and macroscopic scales, while the application of methods of the generalized kinetic theory is in progress. Therefore, the presentation of this topic is limited to focusing on some guidelines to the modeling approach [45].

2.3.2. Mean field game

The mean field theory was introduced by Lasry and Lions in [46]. At first, the theory was used to describe economic and financial problems.

Here, we are considering mean field games that are halfway between the mean field theory and the game theory; namely, the model is based on the hypothesis of the rationality of the agents (pedestrians or vehicles) described.

In [47], the main interest of mean field games is to simplify the interactions between pedestrians. Consequently, the authors derive a continuum formulation of the crowd dynamics and nonlinear systems involving partial differential equations of crowd models.

In [48], a mean field game approach modeling congestion and aversion in pedestrian crowds is devised.

In [49], an example of a mean field game model for pedestrians with a nonlinear mobility is proposed.

3. Advantages and disadvantages

Each modeling approach presents advantages and limitations, which are summarized below.

The macroscopic approach is not very accurate in the description but is suitable for computational cost and fast simulations. In particular, fluid dynamics models have the advantage of being computationally inexpensive, but they lose something in terms of a detailed description of the situation. They deal with macroscopic quantities, it is to say, mean or average quantities that do not take into account the nature of a single vehicle or pedestrian in a traffic simulation.

The microscopic models are very accurate but very expensive from a computational point of view. In particular, cellular automata are based on rules of behavior and not on equations. This aspect could be considered an advantage because it could simplify the description of the phenomena occurring in the streets. On the other hand, they furnish a discrete idealization of the PDEs and through this idealization, the description could be less realistic. In particular, force based models are detailed but they do not consider the chaotic description of the street phenomena and vehicle and/or pedestrian movement. Furthermore, they are computationally expensive, because they describe the dynamic of each pedestrian or vehicle by ODEs. For this reason, the number of equations could be very high to be simulated in a short time.

The mesoscopic approach is convenient because, on one hand, the description takes into account the microscopic nature of the agents in the model from which a distribution function is deduced; and on the other hand, the macroscopic quantities can be obtained by properly integrating the distribution function.

In particular, for mean field games, the advantage is the utilization of the mean field limit to obtain some average quantities from complex nonlinear PDEs. The hypothesis of rationality considered from the game theory is restrictive and not realistic. One of the criticisms of game theory, as applied to the modeling of human decisions, is that humans are, in practice, rarely fully rational.

Regarding kinetic models, the continuum hypothesis is a bit strong and not realistic, because the cars or pedestrians are not particles in a gas, but their movements are discrete, with spaces between the elements that take part in the street's phenomena and interactions. Moreover, this kind of model can be improved by introducing a granular nature of the flux that mathematically corresponds to the introduction of some class of velocities to which the vehicles belong. In this way, one can be more detailed about the description of vehicle fluxes, and one can overcome the disadvantage of the large amount of time needed to simulate a microscopic model.

4. Riemann problem and Aw-Rascle model

The Aw–Rascle model, grounded in fluid dynamics, represents traffic flow as the motion of a compressible fluid governed by a system of two equations: A conservation law for mass and a conservation law for momentum; therefore, the Aw-Rascle model is called a "second order" model.

In this paper, we investigate the non-homogeneous model presented in [26], which generalizes the original homogeneous model

$$\begin{cases} \frac{\partial \rho}{\partial t} + \frac{\partial(\rho v)}{\partial x} & = 0, \\ \frac{\partial \rho S}{\partial t} + \frac{\partial(\rho v S)}{\partial x} & = \rho G(\rho, S), \end{cases} \tag{4.1}$$

where $\rho(x,t)$ and $v(x,t)$ denote, respectively, the density and the velocity of the cars located at position x and at time t, $S = v + p(\rho)$, where the increasing function $p(\rho)$ is introduced in order to take into account driver's reactions to the state of the traffic in front of them. Moreover, $p(\rho)$ must satisfy the conditions

$$p(0) = 0, \quad \lim_{\rho \to 0} \rho p'(\rho) = 0, \quad \frac{d^2}{d\rho}(\rho p(\rho)) > 0.$$

Here, $G(\rho, S)$ is a relaxation function that takes into account possible entries or exits on the road. The prototypes of the functions $p(\rho)$ and $G(\rho, S)$ considered in [15,26] are: $p(\rho) = \rho^\gamma$; $G = \frac{S}{\tau}$, where $\gamma > 0$, and the relaxation times τ are constants.

System (4.1), according the analysis developed in [27, 28], concerning the differential constraints compatible with the Aw-Rascle system, can be written in the following form:

$$\begin{cases} \frac{\partial \rho}{\partial t} + \lambda^{(1)} \frac{\partial \rho}{\partial x} &= -\rho(k_0 \rho + c_0) g(S), \\ \\ \frac{\partial v}{\partial t} + \lambda^{(1)} \frac{\partial v}{\partial x} &= (c_0 v + c_1) g(S), \end{cases} \tag{4.2}$$

where $\lambda^{(1)} = v(x,t) - \rho(x,t)$ is one of the eigenvalues of the matrix associated with the non-homogeneous Aw-Rascle system (4.1). $g(S)$ is in general, an undefined function that arises from the differential constraints procedure. In this case, however, is expressed as

$$g(S) = S - S_0,$$

where $S(x,t) = \rho(x,t) + v(x,t)$. c_0, k_0, and c_1 are arbitrary constants. Discontinuous initial data are assigned, with jump in $x = 0$, investigating Riemann solutions for the Aw-Rascle model. In this paper, a double discountinuity has been taken into account as follows:

$$\rho(x,0) = \begin{cases} \rho_1, & if \quad x < 0, \\ \rho_2, & if \quad 0 < x < L, \\ \rho_3, & if \quad x > L, \end{cases} \qquad v(x,0) = \begin{cases} v_1, & if \quad x < 0, \\ v_2, & if \quad 0 < x < L, \\ v_3, & if \quad x > L, \end{cases} \tag{4.3}$$

where the constants ρ_i and v_i are such that $\rho_1 < \rho_2$, $\rho_3 < \rho_2$, $v_1 > v_2$, $v_3 > v_2$ and $v_1 + \rho_1 = v_2 + \rho_2 = v_3 + \rho_3$. The analytical solution presented in [27, 28] is reported here for the sake of readability:

If $t < t_c$

$$(\rho(x,t), v(x,t)) = \begin{cases} (\rho_1, v_1), & if \quad x < s_1 t, \\ (\rho_2, v_2), & if \quad s_1 t < x < x_l(t), \\ (\frac{1}{2}(v_1 + \rho_1 - \frac{x-L}{t}), v_2 + \rho_2 - \frac{1}{2}(v_1 + \rho_1 - \frac{x-L}{t})), & if \quad x_l(t) \le x < x_r(t), \\ (\rho_3, v_3), & if \quad x \ge x_r(t), \end{cases} \tag{4.4}$$

where

$$s_1 = v_1 + \frac{\rho_2}{(\rho_2 - \rho_1)}(p_1 - p_2)$$

is the shock velocity, and

$$x_l(t) = (v_2 - \rho_2 p_2')t + L, \quad x_r(t) = (v_3 - \rho_3 p_3')t + L, \quad t_c = \frac{L}{s_1 + \rho_2 p_2' - v_2}.$$

If $t_c < t < \tilde{t}_c$

$$(\rho(x,t), v(x,t)) = \begin{cases} (\rho_1, v_1), & if \quad x < \tilde{x}_s(t), \\ (\frac{1}{2}(v_1 + \rho_1 - \frac{x-L}{t}), v_2 + \rho_2 - \frac{1}{2}(v_1 + \rho_1 - \frac{x-L}{t})), & if \quad \tilde{x}_s(t) \le x < x_r(t), \\ (\rho_3, v_3), & if \quad x \ge x_r(t), \end{cases} \tag{4.5}$$

where

$$\tilde{t}_c = \frac{L^2}{\rho_2 - \rho_1}, \qquad \tilde{x}_s(t) = (v_1 - \rho_1)t - \frac{2L}{\sqrt{t_c}}\sqrt{t} + L.$$

If $t > \tilde{t}_c$

$$(\rho(x,t), v(x,t)) = \begin{cases} (\rho_1, v_1), & if \quad x < s_3(t - \tilde{t}_c) + \tilde{x}_c, \\ (\rho_3, v_3), & if \quad x > s_3(t - \tilde{t}_c) + \tilde{x}_c, \end{cases} \tag{4.6}$$

where

$$s_3 = v_1 - \rho_3, \qquad \tilde{x}_c = \frac{L}{(\rho_3 - \rho_1)^2[(v_3 - \rho_3)(\rho_2 - \rho_1) + (\rho_3 - \rho_1)^2]}.$$

Therefore, several numerical methods such as the Upwind, Lax Wendroff, and Beam Warming methods are proposed for their integration and compared in terms of accuracy.

5. Numerical methods

In this section, the general framework for numerical methods is presented (see [25] for further details about numerical methods). System (4.2) can be written as a hyperbolic system in the following form:

$$\frac{\partial u}{\partial t} + A(u)\frac{\partial u}{\partial x} = B(u),$$

where

$$A(u) = \begin{pmatrix} \lambda^{(1)}(u) & 0 \\ 0 & \lambda^{(1)}(u) \end{pmatrix}, \tag{5.1}$$

$u = (\rho, v)^t$ is the transposed row vector of the independent variables,

$$B(u) = (-\rho(k_0\rho + c_0)g(S), (c_0 v + c_1)g(S))^t$$

is the source term and, $\lambda^{(1)}(u) = v - \rho$.

Let us consider a grid with evenly spaced points $x_j = x_{j-1} + h$, $j = 1, \ldots, J$ and time discretization $t_n = t_{n-1} + k$, $n = 1, \ldots, N$ with the constant time step k. Consequently, we denote with u_j^n the numerical approximation of the the vectorial function $u = u(x,t)$ evaluated in the x_j point at the time t^n.

5.1. Lax Wendroff method

The general Lax Wendroff method, in the homogeneous case and with the A matrix constant, is the following:

$$u_j^{n+1} = u_j^n - \frac{k}{2h}A(u_{j+1}^n - u_{j-1}^n) + \frac{k^2}{2h^2}A^2(u_{j+1}^n - 2u_j^n + u_{j-1}^n). \tag{5.2}$$

In our case, the discretization of the matrix $A(u)$ and the source term $B(u)$ is required. Therefore it reads:

$$u_j^{n+1} = u_j^n - \frac{k}{2h}A_j^n(u_{j+1}^n - u_{j-1}^n) + \frac{k^2}{2h^2}(A_j^n)^2(u_{j+1}^n - 2u_j^n + u_{j-1}^n) + kB_j^n. \tag{5.3}$$

5.2. Upwind method

The Upwind method is based on a first order approximation of the time and space derivatives.

In detail:

If $a_j^n > 0$:

$$u_j^{n+1} = u_j^n - \frac{k}{h}a_j^n(u_j^n - u_{j-1}^n) + kB_j^n, \tag{5.4}$$

if $a_j^n < 0$:

$$u_j^{n+1} = u_j^n - \frac{k}{h}a_j^n(u_{j+1}^n - u_j^n) + kB_j^n, \tag{5.5}$$

where $a_j^n = \lambda^{(1)}(u_j^n)$.

5.3. Beam Warming method

Since the Upwind method is only first order accurate, the Beam Warming method is a good alternative to the Upwind method because it causes the characteristic to vary, depending on the sign of the advection term, but it is second order accurate. The same discretization introduced for the Lax Wendroff method is considered, while taking into account the sign of $a_j^n = \lambda^{(1)}(u_j^n)$.

In detail:

if $a_j^n > 0$:

$$u_j^{n+1} = u_j^n - \frac{k}{2h}a_j^n(3u_j^n - 4u_{j-1}^n + u_{j-2}^n) + \frac{k^2}{2h^2}(a_j^n)^2(u_j^n - 2u_{j-1}^n + u_{j-2}^n) + kB_j^n, \tag{5.6}$$

if $a_j^n < 0$:

$$u_j^{n+1} = u_j^n - \frac{k}{2h}a_j^n(-3u_j^n + 4u_{j+1}^n - u_{j+2}^n) + \frac{k^2}{2h^2}(a_j^n)^2(u_j^n - 2u_{j+1}^n + u_{j+2}^n) + kB_j^n. \tag{5.7}$$

6. Numerical simulations

To proceed with simulations, the parameters appearing in system (4.2) have been chosen as $c_0 = 0.1$, $c_1 = 2$, $k_0 = 0.03$, $L = 3$, while the initial conditions, depicted in Figure 1, are as in [28]:

$$\rho(x,0) = \begin{cases} 13/4, & if \quad x < 0, \\ 7, & if \quad 0 < x < L, \\ 4, & if \quad x > L, \end{cases} \qquad v(x,0) = \begin{cases} 23/4, & if \quad x < 0, \\ 2, & if \quad 0 < x < L, \\ 5, & if \quad x > L. \end{cases} \tag{6.1}$$

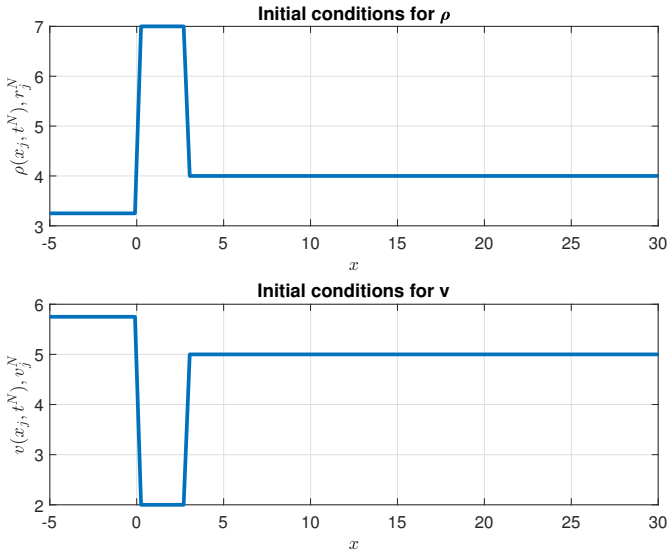

Figure 1. Top: The plot of $\rho(x, 0)$. Bottom: The plot of $v(x, 0)$.

We observe that $v_1 + \rho_1 = v_2 + \rho_2 = v_3 + \rho_3 = 9$. In the following, we present the results for the different numerical schemes. In particular, in Figures 2 and 3, comparisons among the three solutions corresponding to the numerical methods are presented, for fixed time values.

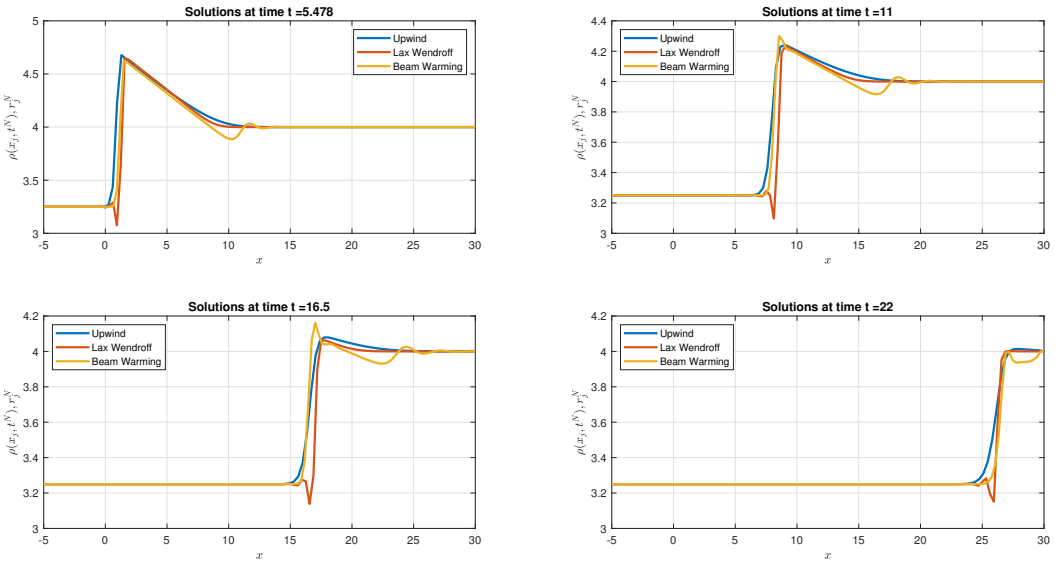

Figure 2. Comparison among numerical solutions for the density. The blue line is the Upwind solution, the orange line is the Lax Wendroff solution, and the yellow line is the Beam Warming solution. Different time steps are considered.

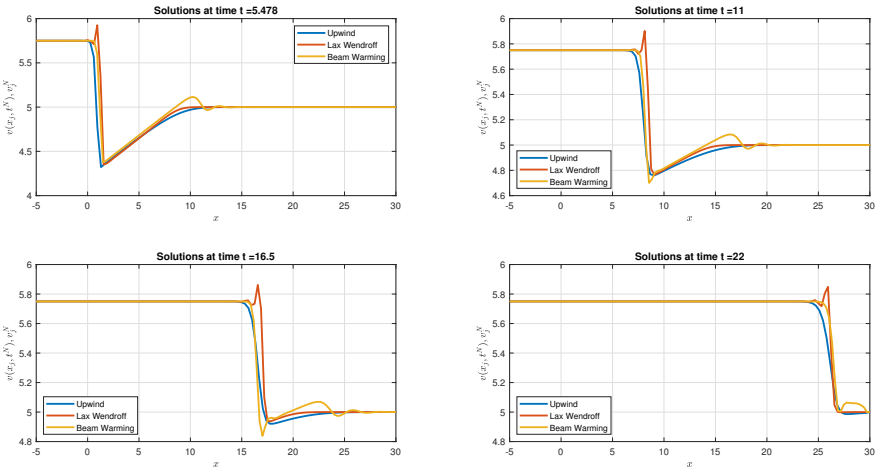

Figure 3. Comparison among numerical solutions for the velocity. The blue line is the Upwind solution, the orange line is the Lax Wendroff solution, and the yellow line is the Beam Warming solution. Different time steps are considered.

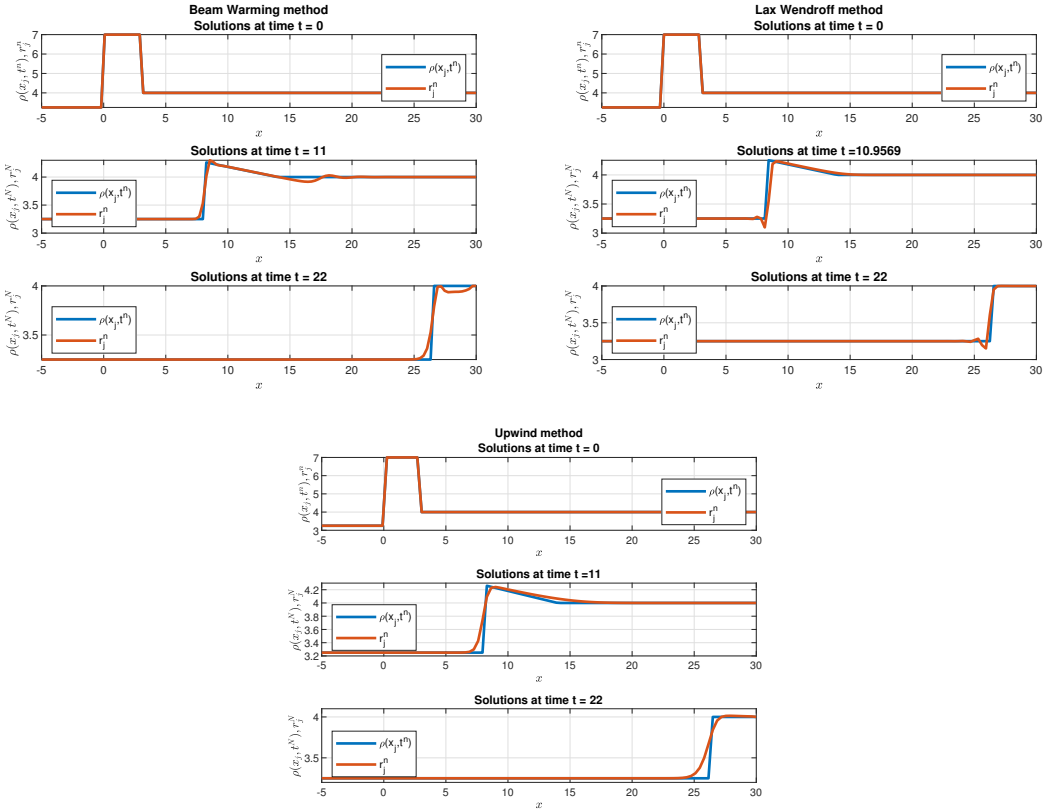

Figure 4. Comparison between exact (blue line) and numerical solution (orange line) calculated by the Beam Warming, Lax Wendroff, and Upwind method, for the density at different time steps.

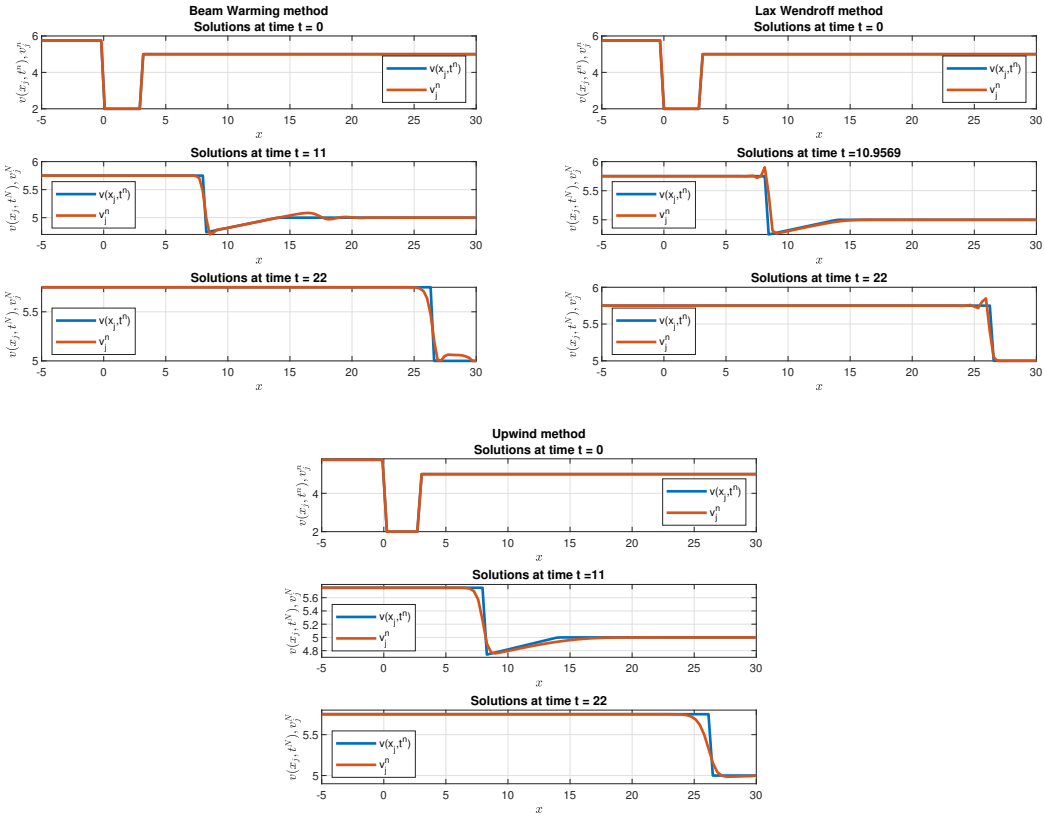

Figure 5. Comparison between exact (blue line) and numerical solution (orange line) calculated by the Beam warming, Lax Wendroff, and Upwind methods, for the velocity at different time steps.

In Figures 4 and 5, a comparison between the exact and numerical solutions for the numerical methods and time steps are depicted. The numerical parameters used for the simulations are: $N_{BW} = 1117$, $J_{BW} = 125$, $N_{LW} = 256$, $J_{LW} = 113$, $N_{UW} = 1001$, $J_{UW} = 101$, which are the numbers of time and space grid points for the Beam Warming method, Lax Wendroff method, and Upwind method, respectively; $x_0 = -5$, $x_{max} = 30$, and $t_{max} = 22$, $dx = \frac{x_{max}-x_0}{(J-1)}$ and $dt = \frac{t_{max}-t_0}{(N-1)}$, where N and J are the numbers of time and space grid points, respectively.

For each numerical method, the CFL condition is satisfied. In particular, since the eigenvalue $\lambda^{(1)}$ is not constant, the CFL condition is defined as

$$c = |\max(\max(\lambda^{(1)}))dt/dx| < 1,$$

and in the following, the values of CFL for each numerical method are listed:

- Beam Warming: $c = 0.17 < 1$;
- Lax Wendroff : $c = 0.78 < 1$;
- Upwind: $c = 0.16 < 1$.

To have some insights on the accuracy of the three compared numerical solutions, we have also plotted the absolute error between the exact and the numerical solution in Figures 6 and 7 for density

and velocity, respectively. For each row of the plot, we consider different time steps: $t = \frac{t_{max}}{4}, \frac{t_{max}}{2}, \frac{3t_{max}}{4}$, and t_{max}.

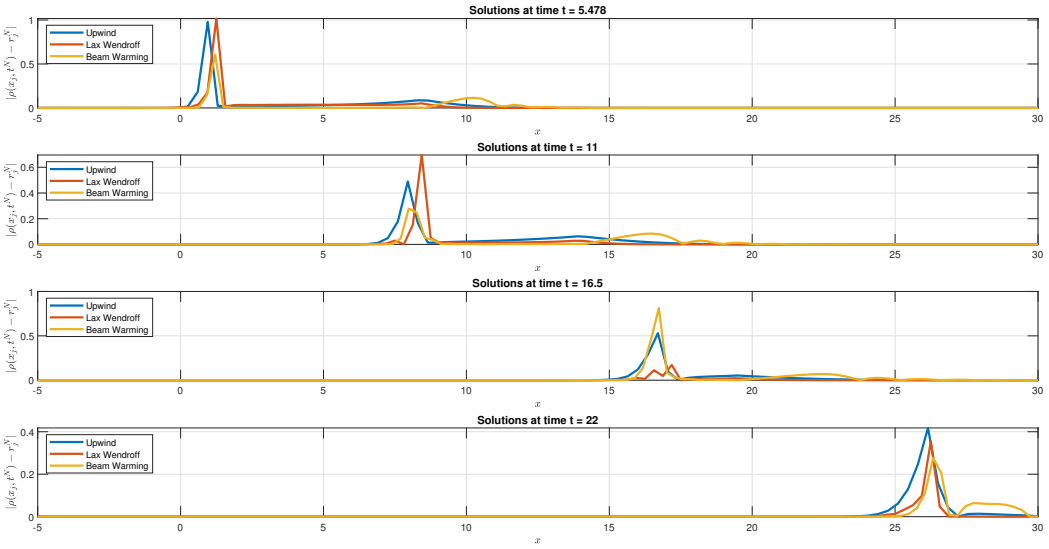

Figure 6. The error $|\rho(x_j, \bar{t}) - r_j^n|$ at different fixed time steps $\bar{t}$ between the exact and numerical solutions, comparing the Upwind method (blue line), the Lax Wendroff method (orange line), and the Beam Warming method (yellow line).

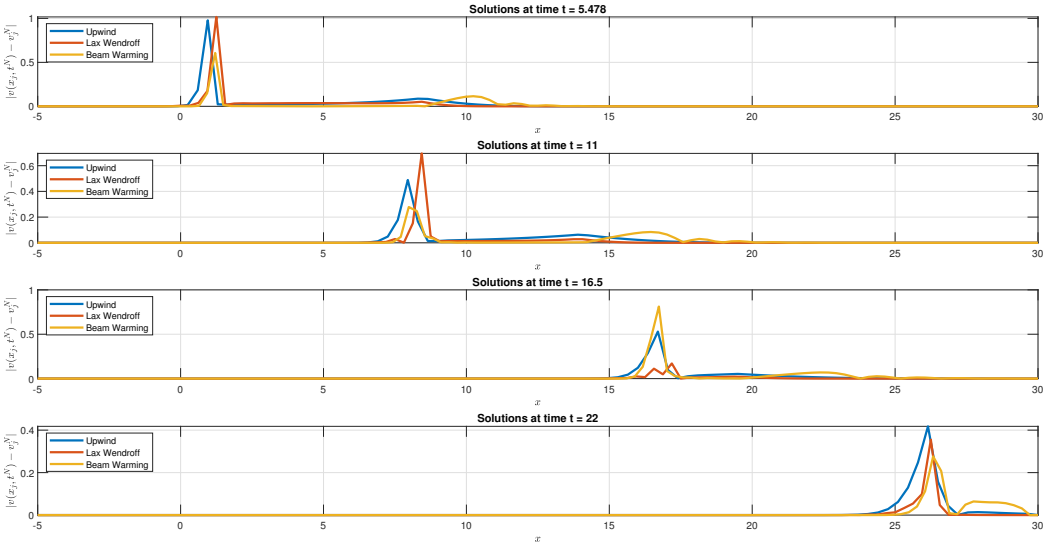

Figure 7. The error $|v(x_j, \bar{t}) - v_j^n|$ at different fixed time steps $\bar{t}$ between the exact and numerical solutions, comparing the Upwind method (blue line), the Lax Wendroff method (orange line), and the Beam Warming method (yellow line).

To have a numerical knowledge of the error analysis, in Table 1

$$Err_1 = \max_j |u(x_j, \bar{t}) - u_j^n|$$

is reported, and in Table 2, the relative norm 2 error is calculated

$$Err_2 = \frac{\sqrt{\sum_j |u(x_j, \bar{t}) - u_j^n|^2}}{\sqrt{\sum_j |u(x_j, \bar{t})|^2}},$$

to have an idea of the error in relation with the exact solution. These results show that the best approach to apply is the Beam Warming method.

Table 1. Norm 1 error for density (top) and for velocity (bottom), at fixed time steps and for numerical methods.

$\mathbf{Err_1}\ \rho$	t = $t_{max}/4$	t=$t_{max}/2$	$t = 3t_{max}/4$	t =t_{max}
Lax Wendroff	1.01	0.7	0.17	0.36
Beam Warming	0.60	0.28	0.81	0.28
Upwind	0.98	0.49	0.53	0.42
$\mathbf{Err_1}\ v$	t = $t_{max}/4$	t=$t_{max}/2$	$t = 3t_{max}/4$	t =t_{max}
Lax Wendroff	1.02	0.7	0.17	0.36
Beam Warming	0.60	0.28	0.81	0.28
Upwind	0.98	0.49	0.53	0.42

Table 2. Relative norm 2 error with respect to the exact solution for density (top) and for velocity (bottom), at fixed time steps and for numerical methods.

$\mathbf{Err_2}\ \rho$	t = $t_{max}/4$	t=$t_{max}/2$	$t = 3t_{max}/4$	t =t_{max}
Lax Wendroff	0.02	0.02	0.01	0.01
Beam Warming	0.02	0.01	0.03	0.01
Upwind	0.03	0.02	0.02	0.02
$\mathbf{Err_2}\ v$	t = $t_{max}/4$	t=$t_{max}/2$	$t = 3t_{max}/4$	t =t_{max}
Lax Wendroff	0.02	0.01	0.00	0.01
Beam Warming	0.01	0.01	0.02	0.01
Upwind	0.02	0.01	0.01	0.01

6.1. New cases

In this subsection, examples are given, by changing the initial conditions with respect to [28], to validate our approach. The new initial conditions considered are the following:

$$\rho(x,0) = \begin{cases} 1/2, & if \quad x < 0, \\ 1, & if \quad 0 < x < L, \\ 1/3, & if \quad x > L, \end{cases} \qquad v(x,0) = \begin{cases} 99.5, & if \quad x < 0, \\ 99, & if \quad 0 < x < L, \\ 99.66, & if \quad x > L. \end{cases} \tag{6.2}$$

In Figures 8 and 9, a comparison between the exact and numerical solutions for the different numerical methods and for different time steps are depicted. The numerical parameters used for the simulations are $N_{BW} = 106$, $J_{BW} = 129$, $N_{LW} = 104$, $J_{LW} = 126$, $N_{UW} = 100$, $J_{UW} = 121$, with the same notation used previously.

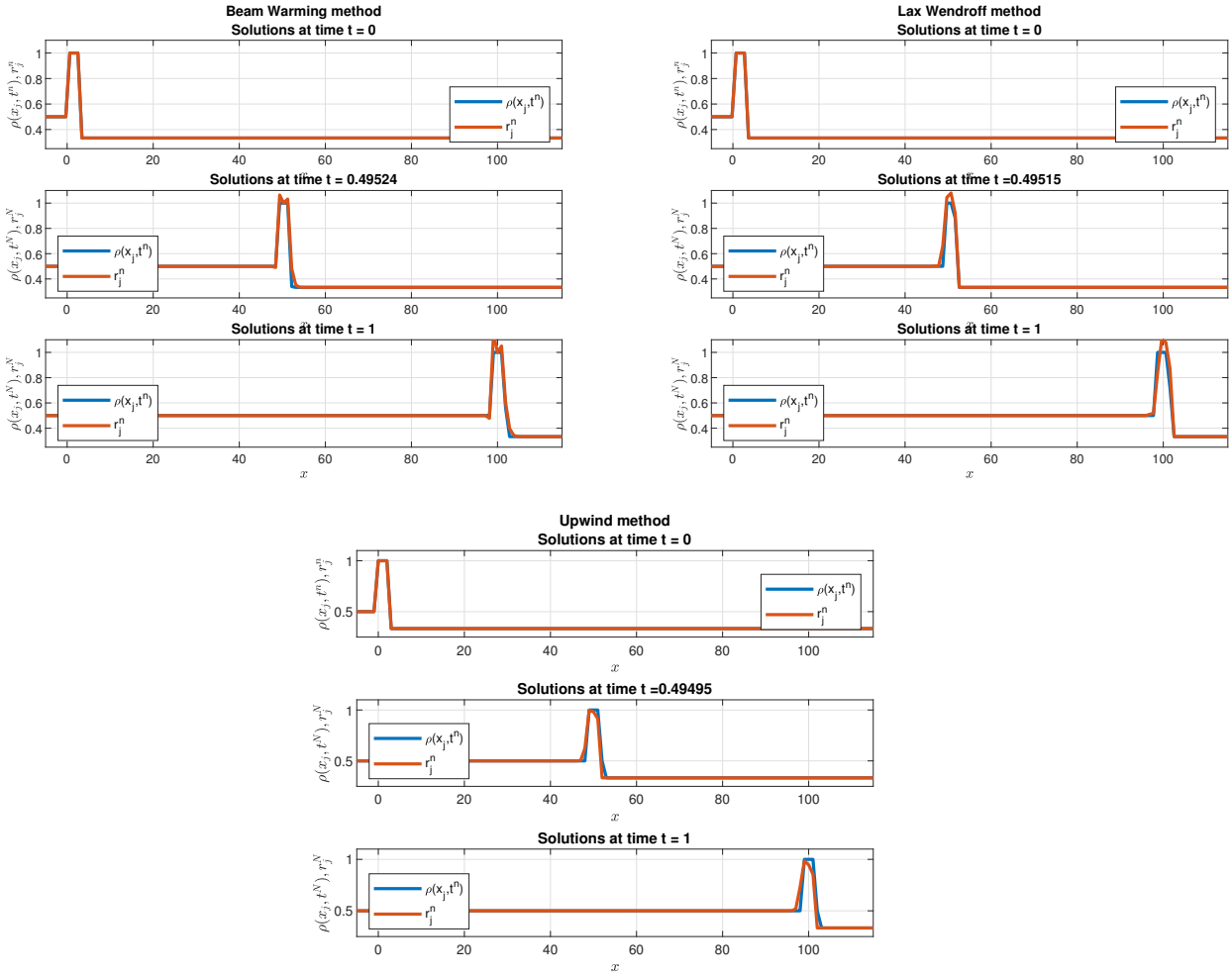

Figure 8. Comparison between exact (blue line) and numerical solutions (orange line) calculated by the Beam Warming, Lax Wendroff, and Upwind methods, for the density at different time steps.

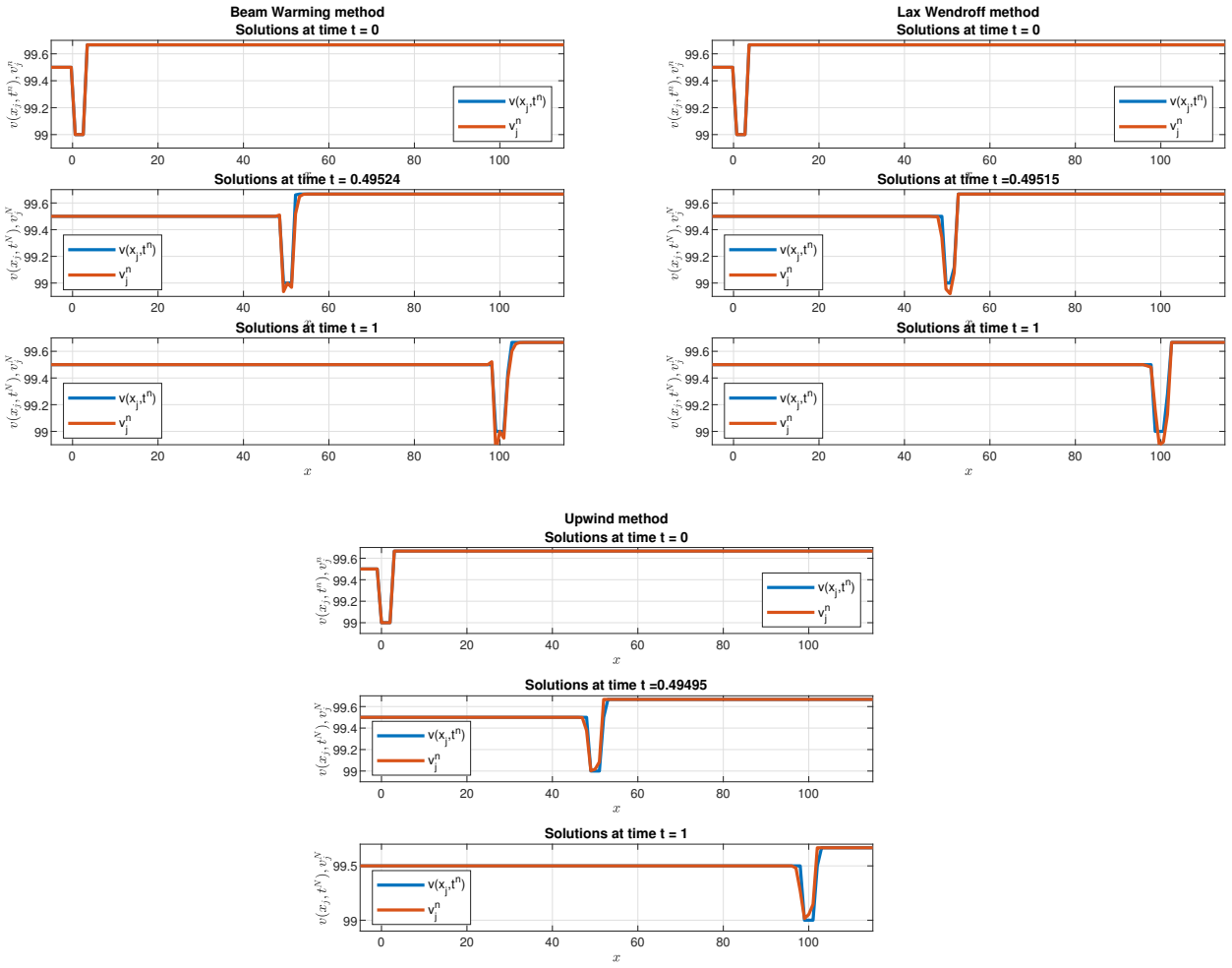

Figure 9. Comparison between exact (blue line) and numerical solutions (orange line) calculated by the Beam warming, Lax Wendroff, and Upwind methods, for the velocity at different time steps.

The plots indicate that the best method is the Beam Warming method. To be more precise, the errors Err_1 and Err_2 are reported in Tables 3 and 4.

Table 3. Norm 1 error for density (top) and for velocity (bottom), at fixed time steps and for numerical methods.

Err$_1$ ρ	t = $t_{max}/4$	t=$t_{max}/2$	$t = 3t_{max}/4$	t =t_{max}
Lax Wendroff	0.08	0.16	0.25	0.16
Beam Warming	0.08	0.14	0.10	0.14
Upwind	0.17	0.17	0.18	0.23
Err$_1$ v	t = $t_{max}/4$	t=$t_{max}/2$	$t = 3t_{max}/4$	t =t_{max}
Lax Wendroff	0.08	0.16	0.25	0.16
Beam Warming	0.08	0.14	0.10	0.14
Upwind	0.17	0.17	0.18	0.23

Table 4. Relative norm 2 error with respect to the exact solution for density (top) and for velocity (bottom), at fixed time steps and for numerical methods.

$\mathbf{Err_2}\ \rho$	t = $t_{max}/4$	t=$t_{max}/2$	$t = 3t_{max}/4$	t =t_{max}
Lax Wendroff	0.02	0.04	0.06	0.05
Beam Warming	0.02	0.03	0.02	0.03
Upwind	0.04	0.05	0.05	0.06
$\mathbf{Err_2}\ v$	t = $t_{max}/4$	t=$t_{max}/2$	$t = 3t_{max}/4$	t =t_{max}
Lax Wendroff	9e-05	2e-04	3e-04	2e-04
Beam Warming	8e-05	1e-04	1e-04	2e-04
Upwind	2e-04	2e-04	3e-04	3e-04

Since we are interested in applying these to the traffic flow simulation, we want to analyze the case in which the traffic light problem is included; when $\rho_2 = v_1$ so that $v_1 > \rho_1$, then $s_1 = 0$ and $x_c = 0$. In this case, the shock originated in $x = 0$ is stationary, while the second shock formed at $t = t_c$ propagates forward. In detail, for the traffic light problem, the initial conditions are $\rho_1 = \rho_3 = 0$, $\rho_2 = \rho_{max}$, $v_1 = v_3 = v_{max}$, $v_2 = 0$, with ρ_{max} and v_{max} denoting, the maximum density and the maximum velocity, respectively. The initial data of the generalized Riemann problem can model a situation where at $t = 0$, a queue of cars localized in $[0, L]$ starts to move. In particular, for the traffic light case, in $x = L$, there is a red traffic light which at $t = 0$ switches to green. Figures 10 and 11 show a comparison between the exact and numerical solutions for the distinct numerical methods and time steps are depicted. The numerical parameters used in this case are the following:

- $\rho_{max} = 15$;
- $v_{max} = 15$;
- x_0 = -5;
- $x_{max} = 115$;
- $t_0 = 0$;
- $t_{max} = 6$;

The initial conditions are:

$$\rho(x,0) = \begin{cases} 0 & if \quad x < 0 \\ \rho_{max} & if \quad 0 < x < L \\ 0 & if \quad x > L \end{cases}, \qquad v(x,0) = \begin{cases} v_{max} & if \quad x < 0 \\ 0 & if \quad 0 < x < L \\ v_{max} & if \quad x > L \end{cases}. \tag{6.3}$$

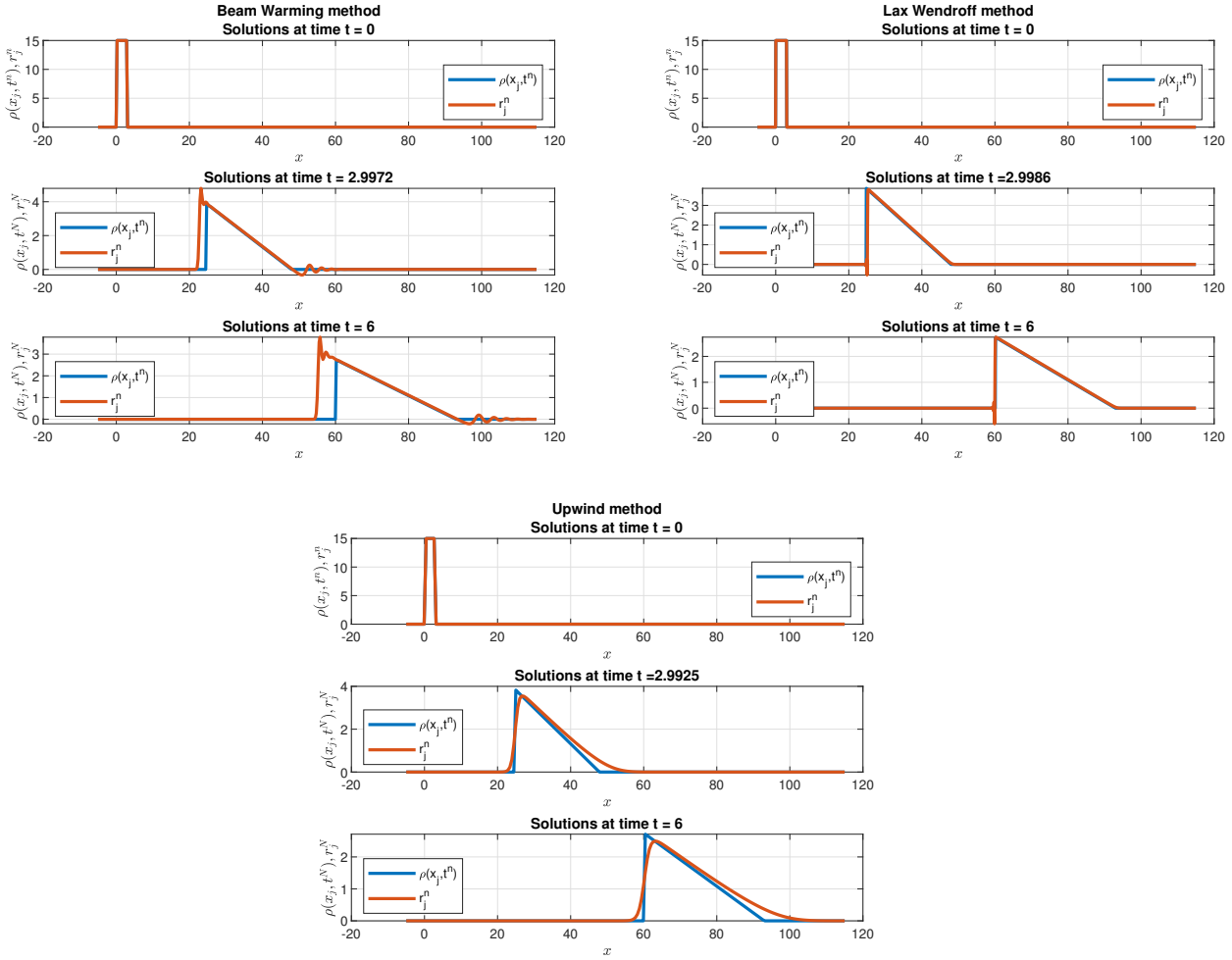

Figure 10. Comparison between exact (blue line) and numerical solutions (orange line) calculated by the Beam Warming, Lax Wendroff, and Upwind methods, for the density at different time steps.

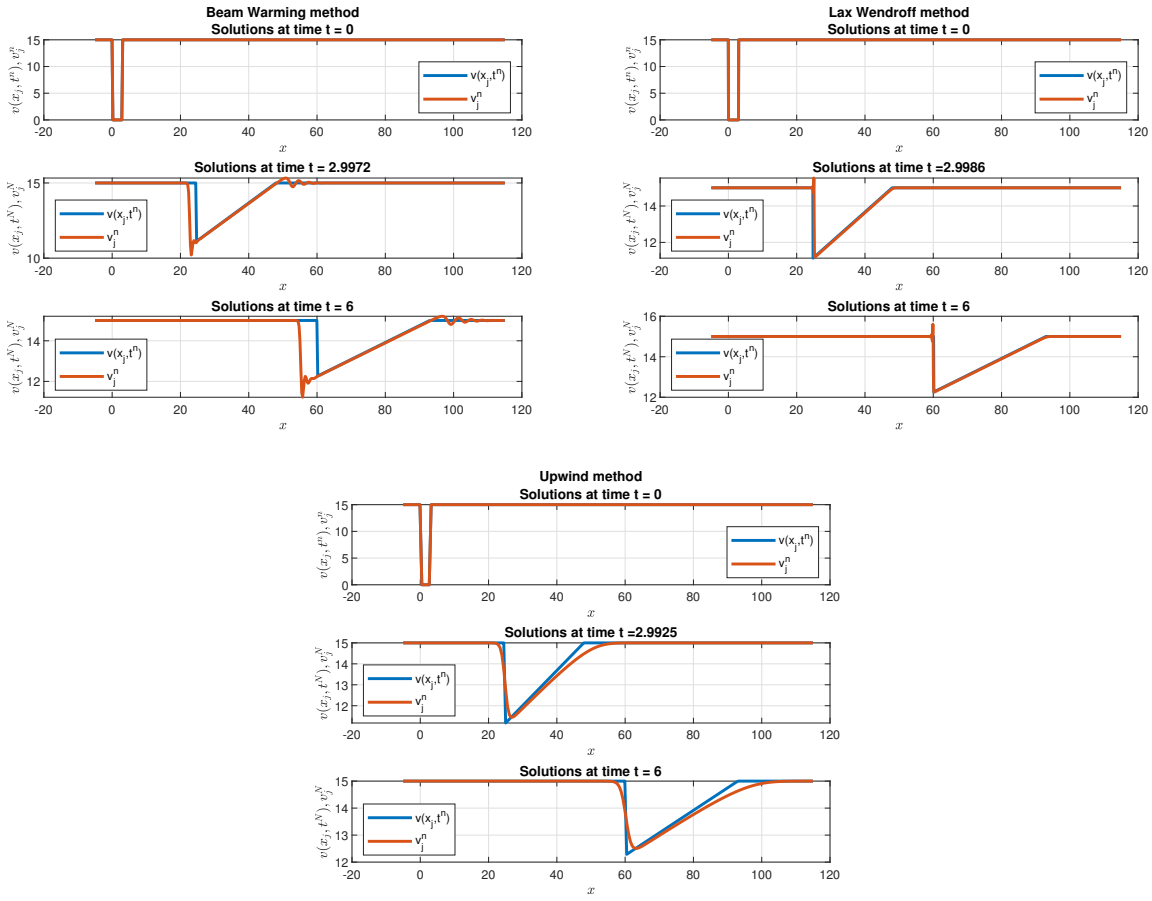

Figure 11. Comparison between exact (blue line) and numerical solutions (orange line) calculated by the Beam Warming, Lax Wendroff, and Upwind methods, for the density at different time steps.

In this last case, the best numerical method is the Lax Wendroff method. To be more precise, the errors Err_1 and Err_2 are reported in Tables 5 and 6. The numerical parameters used for the simulations are $N_{BW} = 1060$, $J_{BW} = 461$, $N_{LW} = 2112$, $J_{LW} = 1765$, $N_{UW} = 400$, $J_{UW} = 221$, with the same notation used previously.

Table 5. Norm 1 error for density (top) and for velocity (bottom), at fixed time steps and for numerical methods.

Err$_1$ ρ	t = $t_{max}/4$	t=$t_{max}/2$	$t = 3t_{max}/4$	t =t_{max}
Lax Wendroff	6.28	4.37	3.82	2.54
Beam Warming	6.00	4.79	4.17	3.78
Upwind	2.65	1.60	1.33	1.18
Err$_1$ v	t = $t_{max}/4$	t=$t_{max}/2$	$t = 3t_{max}/4$	t =t_{max}
Lax Wendroff	6.28	4.37	3.82	2.54
Beam Warming	6.00	4.79	4.17	3.78
Upwind	2.65	1.60	1.33	1.18

Table 6. Relative norm 2 error with respect to the exact solution for density (top) and for velocity (bottom), at fixed time steps and for numerical methods.

$\mathbf{Err_2}\ \rho$	t = $t_{max}/4$	t=$t_{max}/2$	$t = 3t_{max}/4$	t =t_{max}
Lax Wendroff	0.29	0.22	0.13	0.09
Beam Warming	0.35	0.53	0.67	0.73
Upwind	0.22	0.20	0.21	0.21
$\mathbf{Err_2}\ v$	t = $t_{max}/4$	t=$t_{max}/2$	$t = 3t_{max}/4$	t =t_{max}
Lax Wendroff	0.02	0.01	0.01	0.01
Beam Warming	0.03	0.04	0.04	0.04
Upwind	0.02	0.01	0.01	0.01

7. Conclusions

Riemann problem-based approaches are widely employed in traffic flow modeling to analyze wave propagation phenomena and discontinuities arising from conservation laws. Nevertheless, their applicability is subject to several limitations. These models typically rely on idealized assumptions, such as piecewise constant initial conditions and sharp discontinuities, which rarely reflect the continuous and dynamically evolving nature of real traffic states. Moreover, exact analytical solutions are generally restricted to simplified macroscopic formulations with relatively elementary structures, whereas more realistic settings, such as incorporating source terms, heterogeneous road characteristics, driver behavior variability, or external controls, require approximate or fully numerical solvers. Additional challenges emerge when extending the framework to complex urban networks, where junctions, road bifurcations, and signalized intersections necessitate supplementary coupling and priority conditions to regulate flow distribution. Consequently, while Riemann problem formulations provide valuable theoretical insight into fundamental traffic wave dynamics, their direct generalization to large-scale, heterogeneous urban systems remains non-trivial and requires further modeling extensions. If the proposed scheme is extended to a realistic traffic domain, the latter should first be discretized and represented as a mesh. Potential junctions, such as road bifurcations or signalized intersections, should be explicitly identified as marked nodes of the grid. Each one, treated either in parallel (for multiple interacting branches) or sequentially in the case of a unidirectional road, can be formulated as a local Riemann problem governing the interaction of incoming and outgoing flows and by using coupled through time-dependent boundary conditions, which regulate the exchange of fluxes between adjacent cells and enable the incorporation of dynamic control mechanisms, such as traffic signals or varying demand patterns.

In this study, three numerical methods are compared. Moreover, the Upwind, Beam–Warming, and Lax–Wendroff methods are applied to the non-homogeneous Aw–Rascle model with discontinuous initial conditions (Generalized Riemann Problem). Since the exact solution is available, it is used as a benchmark to assess the accuracy of the numerical approximations.

The results show that this analysis can be useful in situations where the exact solution is not available, to select the most appropriate numerical approach. In particular, the Beam–Warming method proves to be the most accurate in some cases, while the Lax–Wendroff method performs better in others.

Author contributions

All authors contributed equally to this article. All authors have read and agreed to the published version of the manuscript.

Use of Generative-AI tools declaration

The authors declare they have not used Artificial Intelligence (AI) tools in the creation of this article.

Acknowledgement

This research was granted by PNRR-M4C2- I1.1 – MUR Call for proposals n.104 of 02-02-2022 - PRIN 2022 – ERC sector SH7- Project title: MOVING StEPS - MOVING from Street Experiments to adaptive Planned Solutions - Project Code 2022BLK9TS - CUP Code J53D23009280008 - Funded by the European Union – NextGenerationEU. Manuscript developed within the PRIN 2022 "URGET VADEMECUM 2030-50 - URban de-pollution and de-carbonisation from emissions GEnerated by Transport systems: eVAluation of DEdicated Methodologies, technologies and EConomic thresholds for an Unprecedented Mobility at 2030-50. Research project funded by: Ministry of Scientific Research; Italia Domani - National Recovery and Resilience Plan; European Union - Next Generation EU. The authors A. R., M. R, G. V. acknowledge the support by G.N.F.M. of I.N.d.A.M.

Conflict of interest

Marianna Ruggieri is the Guest Editor of special issue "Advanced in Nonlinear Differential Equations: Theory, Methods and Applications" for AIMS Mathematics. Marianna Ruggieri was not involved in the editorial review and the decision to publish this article.

References

1. S. P. Sathiyan, C. B, Pratap, A. A. Stonier, G. Peter, A. Sherine, K. Praghash, Comprehensive assessment of electric vehicle development, deployment, and policy initiatives to reduce GHG emissions: Opportunities and challenges, *IEEE Access*, **10** (2022), 53614–53639. https://doi.org/10.1109/ACCESS.2022.3175585
2. G. Acampa, A. Pino, F. Alberti, G. Rossi, The URGET VADEMECUM 2030–2050 project: Applying threshold theory to sustainable urban mobility, In: *Networks, markets & people, Lecture notes in networks and systems*, 2024, 172–181. https://doi.org/10.1007/978-3-031-74679-6_17
3. A. Ricciardello, M. Ruggieri, C. Scuro, *Predictive modeling for urban dynamics*, In: 2026 IEEE International Workshop on Metrology for Living Environment (MetroLivEnv), Cambridge, 2026.
4. E. Mustafa, H. Özen, Developing a sustainable urban mobility maturity model, *Sustainability*, **18** (2026), 689. https://doi.org/10.3390/su18020689
5. T. Campisi, A. Ricciardello, M. Ruggieri, G. Vitanza, *A preliminary analysis on parklets: Can they contribute to the realisation of a walking friendly city in italy*? In: ICCSA 2024 Workshops, ICCSA 2024, Lecture Notes in Computer Science, Springer, Cham., **14823** (2024), 168–183. https://doi.org/10.1007/978-3-031-65329-2_11

6. T. Li, Y. Luo, X. Wan, Q. Li, Q. L. Liu, R. Wang, et al., A malware detection model based on imbalanced heterogeneous graph embeddings, *Expert Syst. Appl.*, **246** (2024), 123109. https://doi.org/10.1016/j.eswa.2023.123109
7. A. Anuradha, A. S. Chouhan, S. S. Rao, Improving malware detection performance using hybrid deep representation learning with heuristic search algorithms, *Sci. Rep.*, **16** (2026), 4847. https://doi.org/10.1038/s41598-026-35481-x
8. B. Piccoli, A. Tosin, *Vehicular traffic: A review of continuum mathematical models*, In: Encyclopedia of complexity and systems science, 2009, 9727–9749. https://doi.org/10.1007/978-0-387-30440-3_576
9. N. Chaudhuri, P. Gwiazda, E. Zatorska, Analysis of the generalized Aw-Rascle model, *Commun. Part. Diff. Eq.*, **48** (2023), 440–477. https://doi.org/10.1080/03605302.2023.2183511
10. M. J. Lighthill, G. B. Whitham, On kinematic waves II. A theory of traffic flow on long crowded roads, *Proc. A*, **229** (1955), 317–345. https://doi.org/10.1098/rspa.1955.0089
11. P. I. Richards, Shock waves on the highway, *Oper. Res.*, **4** (1956), 42–51. https://doi.org/10.1287/opre.4.1.42
12. R. L. Hughes, A continuum theory for the flow of pedestrians, *Transport. Res. B-Meth.*, **36** (2002), 507–535. https://doi.org/10.1016/S0191-2615(01)00015-7
13. R. M. Colombo, M. Garavello, M. L. Mercier, A class of nonlocal models for pedestrian traffic, *Math. Mod. Meth. Appl. S.*, **22** (2012), 1150023. https://doi.org/10.1142/S0218202511500230
14. P. Goatin, R. M. Colombo, M. D. Rosini, *A macroscopic model for pedestrian flows in panic situations*, In: 4th Polish-Japan Days, 2009, Madralin, Poland, **32** (2009), 255–272.
15. A. AW, M. Rascle, Resurrection of "second order" models of traffic flow, *SIAM J. Appl. Math.*, **60** (2000), 916–938. https://doi.org/10.1137/S0036139997332099
16. C. A. Rolland, P. Degond, S. Motsch, Two-way multi-lane traffic model for pedestrians in corridors, *Netw. Heterog. Media*, **6** (2011), 351–381. https://doi.org/10.3934/nhm.2011.6.351
17. P. Degond, C. A. Rolland, J. Pettré, G. Theraulaz, Vision-based macroscopic pedestrian models, Kinetic and Related models, *Kinet. Relat. Mod.*, **6** (2013), 809–839. https://doi.org/10.3934/krm.2013.6.809
18. J. Ondřej, J. Pettré, A. H. Olivier, S. Donikian, A synthetic-vision based steering approach for crowd simulation, *ACM T. Graphic.*, **29** (2010), 1–9. https://doi.org/10.1145/1778765.1778860
19. N. K. Mahato, A. Klar, S. Tiwari, A meshfree particle method for a vision-based macroscopic pedestrian model, *Int. J. Adv. Eng. Sci. Ap.*, **10** (2018), 41–53. https://doi.org/10.1007/s12572-018-0204-2
20. J. V. Neumann, A. W. Burks, Theory of self-reproducing automata, 1966.
21. M. Gardner, Mathematical games, *Sci. Am.*, **222** (1970), 132–140. https://doi.org/10.1038/scientificamerican1070-120
22. J. Felcman, P. Kubera, A cellular automaton model for a pedestrian flow problem, *Math. Model. Nat. Pheno.*, **16** (2021), 11. https://doi.org/10.1051/mmnp/2021002
23. Y. Li, M. Y. Chen, Z. Dou, X. P. Zheng, Y. Cheng, A. Mebarki, A review of cellular automata models for crowd evacuation, *Physica A*, **526** (2019), 120752. https://doi.org/10.1016/j.physa.2019.03.117

24. K. Nagel, M. Schreckenberg, A cellular automaton model for freeway traffic, *J. Phys. I*, **2** (1992), 2221–2229. https://doi.org/10.1051/jp1:1992277
25. R. J. LeVeque, *Numerical methods for conservation laws*, Basel: Birkhäuser, 1992. https://doi.org/10.1007/978-3-0348-8629-1
26. S. Gerster, M. Herty, E.Iacomini, Stability analysis of a hyperbolic stochastic Galerkin formulation for the Aw-Rascle-Zhang model with relaxation, *Math. Biosci. Eng.*, **18** (2021), 4372–4389. https://doi.org/10.3934/mbe.2021220
27. C. Curró, N. Manganaro, Riemann problems and exact solutions to a traffic flow model, *J. Math. Phys.*, **54** (2013), 071503. https://doi.org/10.1063/1.4813473
28. A. Jannelli, N. Manganaro, A. Rizzo, Riemann problems for the nonhomogeneous Aw-Rascle model, *Commun. Nonlinear Sci.*, **118** (2023), 107010. https://doi.org/10.1016/j.cnsns.2022.107010
29. D. Ding, Modeling and simulation of highway traffic using a cellular automaton approach, 2011.
30. Y. Xue, L. Y. Dong, L. Li, S. Q. Dai, Effects of changing orders in the update rules on traffic flow, *Phys. Rev. E*, **71** (2005), 026123. https://doi.org/10.1103/PhysRevE.71.026123
31. R. G. N. Lakmali, P. V. Genovese, A. A. B. D. P. Abewardhana, Evaluating the efficacy of agent-based modeling in analyzing pedestrian dynamics within the Built environment: A comprehensive systematic literature review, *Buildings*, **14** (2024), 1945. https://doi.org/10.3390/buildings14071945
32. D. Helbing, A mathematical model for the behavior of pedestrians, *Behav. Sci.*, **36** (1991), 298–310. https://doi.org/10.1002/bs.3830360405
33. D. Helbing, I. Farkas, T. Vicsek, Simulating dynamical features of escape panic, *Nature*, **407** (2000), 487–490. https://doi.org/10.1038/35035023
34. A. Schadschneider, W. Klingsch, H. Kluepfel, T. Kretz, C. Rogsch, A. Seyfried, Evacuation dynamics: Empirical results, modeling and applications, *arXiv Preprint*, 2008. https://doi.org/10.48550/arXiv.0802.1620
35. D.Helbing, P. Molnar, Social force model for pedestrian dynamics, *Phys. Rev. E*, **51** (1995), 4282. https://doi.org/10.1103/PhysRevE.51.4282
36. X. Chen, M. Treiber, V. Kanagaraj, H. Y. Li, Social force models for pedestrian traffic-state of the art, *Transport Rev.*, **38** (2018), 625–653. https://doi.org/10.1080/01441647.2017.1396265
37. M. Chraibi, U. Kemloh, A. Schadschneider, A. Seyfried, Force-based models of pedestrian dynamics, *Netw. Heterog. Media*, **6** (2011), 425–442. https://doi.org/10.3934/nhm.2011.6.425
38. R. Korbmacher, A. Nicolas, A. Tordeux, C. Totzeck, *Time-continuous microscopic pedestrian models: An overview*, In: Crowd dynamics, analytics and human factors in crowd modeling, Birkhäuser, Cham, **4** (2023), 55–80. https://doi.org/10.1007/978-3-031-46359-4_3
39. I. Prigogine, A Boltzmann-like approach to the statistical theory of traffic flow, *Theory Traffic Flow*, 1961.
40. M. Delitala, A. Tosin, Mathematical modeling of vehicular traffic: A discrete kinetic theory approach, *Math. Mod. Meth. Appl. S.*, **17** (2007), 901–932. https://doi.org/10.1142/S0218202507002157
41. L. Fermo, A. Tosin, A fully-discrete-state kinetic theory approach to modeling vehicular traffic, *SIAM J. Appl. Math.*, **73** (2013), 1533–1556. https://doi.org/10.1137/120897110

42. C. F. Daganzo, Requiem for second-order fluid approximations of traffic flow, *Transport. Res. B-Meth.*, **29** (1995), 277–286. https://doi.org/10.1016/0191-2615(95)00007-Z
43. P. J. Shang, M. Wan, S. Kama, Fractal nature of highway traffic data, *Comput. Math. Appl.*, **54** (2007), 107–116. https://doi.org/10.1016/j.camwa.2006.07.017
44. K. Axel, R. Wegener, *Kinetic traffic flow models*, In: Modeling in applied sciences, Boston, MA: Birkhäuser Boston, 2000, 263–316. https://doi.org/10.1007/978-1-4612-0513-5_8
45. N. Bellomo, C. Dogbe, On the modeling of traffic and crowds: A survey of models, speculations, and perspectives, *SIAM Rev.*, **53** (2011), 409–463. https://doi.org/10.1137/090746677
46. J. M. Lasry, P. L. Lions, Mean field games, *Jpn J. Math.*, **2** (2007), 229–260. https://doi.org/10.1007/s11537-007-0657-8
47. C. Dogbé, Modeling crowd dynamics by the mean-field limit approach, *Math. Comput. Model.*, **52** (2010), 1506–1520. https://doi.org/10.1016/j.mcm.2010.06.012
48. A. Lachapelle, M. T. Wolfram, On a mean field game approach modeling congestion and aversion in pedestrian crowds, *Transport. Res. B-Meth.*, **45** (2011), 1572–1589. https://doi.org/10.1016/j.trb.2011.07.011
49. M. Burger, M. D. Francesco, P. Markowich, M. T. Wolfram, Mean field games with nonlinear mobilities in pedestrian dynamics, *arXiv Preprint*, 2013. https://doi.org/10.48550/arXiv.1304.5201

AIMS Press